

Quasiparticle Decoherence in d -wave Superconducting Qubits

M. H. S. Amin and A. Yu. Smirnov

D-Wave Systems Inc., 320-1985 W. Broadway, Vancouver, B.C., V6J 4Y3 Canada

It is usually argued that the presence of gapless quasiparticle excitations at the nodes of the d -wave superconducting gap should strongly decohere the quantum states of a d -wave qubit, making quantum effects practically unobservable. Using a self-consistent linear response non-equilibrium quasiclassical formalism, we show that this is not necessarily true. We find quasiparticle conductance of a d -wave grain boundary junction to be strongly phase dependent. Midgap states as well as nodal quasiparticles contribute to the conductance and therefore decoherence. Quantum behavior is estimated to be detectable in a qubit containing a d -wave junction with appropriate parameters.

Among numerous qubit implementations, superconducting ones enjoy long decoherence times because of their gapped electronic excitation spectrum. This fact has recently been confirmed by several striking experiments [1]. The key constituents in all of those are Josephson tunnel junctions. One advantage of the tunnel junctions is the exponential dependence of their quasiparticle resistance R on temperature T (i.e. $R \sim e^{\Delta/T}$ where Δ is the superconducting gap. Herein $k_B = \hbar = 1$). The electronic decoherence is therefore exponentially suppressed at low T . Similar behavior also exists in superconducting point contacts, with the energy of Andreev levels $\epsilon_0(\phi) = \Delta \cos \phi/2$, replacing Δ in the exponent [2, 3]. Deviation from the exponential dependence is expected at low temperatures [3].

Despite their naturally degenerate ground states [4], desirable for quantum computation, d -wave qubits [5, 6] are controversial because their quasiparticle spectrum is gapless at the nodes of the order parameter. Moreover, experimentally, the normal resistance extracted from I-V characteristics of d -wave grain boundary junctions is found to be very small [7, 8] (with $RC \sim 1$ ps [8]); much smaller than required to observe quantum effects. However, the resistance is measured in the running state of the junctions. The Doppler shift due to large superconducting current in such a state will populate the nodes, enhancing the conductance G ($\equiv 1/R$). Moreover, time variation of the phase difference across the junction would effectively *phase average* G . As we shall see, midgap states (MGS) can significantly contribute to such an averaged G , except at very low T .

The first step is therefore to calculate G for a d -wave grain boundary junction. Most existing methods can study ac properties of a Josephson junction biased with a constant voltage (see e.g. [9, 10]). This however implies a constant variation of phase difference ϕ , which is not the case in qubits. In Ref. 3, a self-consistent non-equilibrium quasiclassical technique was developed to calculate linear response of a Josephson junction to an ac voltage with arbitrary frequency. The method was successfully applied to the case of a superconducting point contact. In high T_c superconductors, the relatively large T_c/E_F (E_F is the Fermi energy), makes the quasiclassical approxi-

mation only marginally applicable. It nevertheless has proven successful in calculating equilibrium properties of d -wave superconductors [11, 12, 13]. Here, we employ the theory of Ref. 3 to calculate G , and therefore decoherence, in a d -wave grain boundary junction.

Let us now briefly describe the technique. More details are provided in Ref. 3. We calculate quasiclassical retarded, advanced, and Keldysh Green's functions [3, 16]

$$\hat{g}^{R,A} = \begin{pmatrix} g^{R,A} & f^{R,A} \\ f^{\dagger R,A} & -g^{\dagger R,A} \end{pmatrix}, \quad \hat{g}^K = \begin{pmatrix} g^K & f^K \\ -f^{\dagger K} & g^{\dagger K} \end{pmatrix},$$

which are functions of the Fermi velocity \mathbf{v}_F , quasiparticle energy ϵ , position \mathbf{r} , and time t . Here $f^{\dagger R}(\mathbf{v}_F, \epsilon; \mathbf{r}, t) \equiv f^R(-\mathbf{v}_F, -\epsilon; \mathbf{r}, t)^*$, etc. In equilibrium, the retarded and advanced Green's functions can be written in terms of Riccati amplitudes [12] a_0^α and b_0^α in a way very similar to the conventional method for the Matsubara Green's functions [12, 13]:

$$g_0^\alpha = s^\alpha \frac{1 - a_0^\alpha b_0^\alpha}{1 + a_0^\alpha b_0^\alpha}, \quad f_0^\alpha = s^\alpha \frac{2a_0^\alpha}{1 + a_0^\alpha b_0^\alpha}, \quad (1)$$

where $\alpha = R, A$ for retarded and advanced functions respectively, and $s^\alpha = + (-)$ for $\alpha = R (A)$. The subscript "0" denotes equilibrium quantities. The amplitudes satisfy Riccati-type equations

$$\begin{aligned} \mathbf{v}_F \cdot \nabla a_0^\alpha &= 2i\epsilon^\alpha a_0^\alpha - (a_0^\alpha)^2 \Delta_0^* + \Delta_0, \\ -\mathbf{v}_F \cdot \nabla b_0^\alpha &= 2i\epsilon^\alpha b_0^\alpha - (b_0^\alpha)^2 \Delta_0 + \Delta_0^*, \end{aligned} \quad (2)$$

where $\epsilon^\alpha = \epsilon + is^\alpha \eta$, with ϵ and η being the real and imaginary parts of the quasiparticle energy respectively. In d -wave superconductors, η results from both inelastic and impurity scattering processes [14]. The boundary conditions are the bulk solutions of (2): $a_0^\alpha = \Delta_0 / (-i\epsilon^\alpha + s^\alpha \Omega^\alpha)$ and $b_0^\alpha = \Delta_0^* / (-i\epsilon^\alpha + s^\alpha \Omega^\alpha)$, where $\Omega^\alpha = \sqrt{|\Delta_0|^2 - (\epsilon^\alpha)^2}$. To calculate a_0^R and b_0^A (b_0^R and a_0^A), we integrate (2) in the direction of \mathbf{v}_F ($-\mathbf{v}_F$), starting from the boundary conditions at $x = -\infty$ ($+\infty$).

Non-equilibrium behavior emerges when an ac voltage $V(t) = V_0 \cos \omega t$ is applied across the junction. Choosing a gauge in which the vector potential $\mathbf{A} = 0$, we consider a scalar potential $\Phi = \pm(V_0/2) \cos \omega t$, with the $+$ ($-$) sign on the left (right) side of the junction. To

ensure applicability of the linear response formalism, it is necessary that $eV_0 \ll \Delta, \omega$ [15].

We define the linear response Green's functions $\delta\hat{g}^\alpha = \hat{g}^\alpha - \hat{g}_0^\alpha$, related to the linear response amplitudes $\delta a^\alpha = a^\alpha - a_0^\alpha$ and $\delta b^\alpha = b^\alpha - b_0^\alpha$ through ($\alpha = R, A$)

$$\delta g^\alpha = -2s^\alpha \frac{\delta a^\alpha b_{0+}^\alpha + \delta b^\alpha a_{0+}^\alpha}{(1 + a_{0+}^\alpha b_{0+}^\alpha)(1 + a_{0-}^\alpha b_{0-}^\alpha)}, \quad (3)$$

$$\delta f^\alpha = 2s^\alpha \frac{\delta a^\alpha - \delta b^\alpha a_{0+}^\alpha a_{0-}^\alpha}{(1 + a_{0+}^\alpha b_{0+}^\alpha)(1 + a_{0-}^\alpha b_{0-}^\alpha)}, \quad (4)$$

where $a_{0\pm}^\alpha \equiv a_0^\alpha(\epsilon \pm \omega/2)$, etc. We also introduce the anomalous Green's function $\delta\hat{g}^X$ (with the same matrix form as \hat{g}^R) by $\delta\hat{g}^K = \delta\hat{g}^X(\mathcal{F}_+ - \mathcal{F}_-) + \delta\hat{g}^R\mathcal{F}_- - \delta\hat{g}^A\mathcal{F}_+$, where $\mathcal{F}_\pm \equiv \tanh[(\epsilon \pm \omega/2)/2T]$. Correspondingly, we introduce anomalous functions δa^X and δb^X which are related to the Green's functions through

$$\delta g^X = 2 \frac{\delta a^X - \delta b^X a_{0+}^R b_{0-}^A}{(1 + a_{0+}^R b_{0+}^R)(1 + a_{0-}^A b_{0-}^A)}, \quad (5)$$

$$\delta f^X = 2 \frac{\delta a^X a_{0-}^A + \delta b^X a_{0+}^R}{(1 + a_{0+}^R b_{0+}^R)(1 + a_{0-}^A b_{0-}^A)}. \quad (6)$$

The differential equations describing δa^α are $\mathbf{v}_F \cdot \nabla \delta a^\alpha = A^\alpha \delta a^\alpha + B^\alpha$, with bulk boundary conditions $\delta a^\alpha = -B^\alpha/A^\alpha$, where

$$A^\alpha = \begin{cases} 2i\epsilon - (a_{0+}^\alpha + a_{0-}^\alpha)\Delta_0^\dagger, & \alpha = R, A \\ i\omega - a_{0+}^R \Delta_0^\dagger + b_{0-}^A \Delta_0, & \alpha = X \end{cases}$$

$$B^\alpha = \begin{cases} \delta\Delta - a_{0+}^\alpha a_{0-}^\alpha \delta\Delta^\dagger - ie\Phi(a_{0+}^\alpha - a_{0-}^\alpha), & \alpha = R, A \\ a_{0+}^R \delta\Delta^\dagger + b_{0-}^A \delta\Delta - ie\Phi(1 + a_{0+}^R b_{0-}^A). & \alpha = X \end{cases}$$

The corresponding equations for δb^α can be obtained by applying a \dagger -operation to both sides of the above equations. Integrations for δa^R , δb^A , and δa^X (δb^R , δa^A , and δb^X) are taken in the direction of \mathbf{v}_F ($-\mathbf{v}_F$), along the quasiclassical trajectories.

The equilibrium order parameter, Δ_0 , is calculated self consistently using numerical iteration, while the linear response $\delta\Delta \equiv \Delta - \Delta_0$ is given by [3]

$$\delta\Delta(\omega) = -2e(\Delta_0/\omega)\Phi(\omega). \quad (7)$$

$\delta\Delta$ satisfies the self-consistency relation up to an error of $O(j_c/j_{c,\text{bulk}})$, where j_c ($j_{c,\text{bulk}}$) is the Josephson (bulk) critical current density. In d -wave grain boundary junctions, $j_c/j_{c,\text{bulk}}$ is smallest for a 0° – 45° junction. Application of (7), instead of common self-consistent iterative methods [16], is a clear advantage of the present technique.

We consider an asymmetric 0° – 45° misoriented d -wave grain boundary junction, with perfect transparency and no roughness. To clearly see the effect of the nodes and bound states, it is useful to define an angle resolved conductance $G_\theta = \text{Re}[\delta j_\theta/V_0]S$, where S is the the area of the junction and

$$\delta j_\theta = \frac{eV_0 N_F}{4} \int_{-\epsilon_c}^{\epsilon_c} d\epsilon \text{Tr} [\hat{\tau}_3 \delta\hat{g}^K]_{\mathbf{v}_F = v_F \hat{\mathbf{n}}} \quad (8)$$

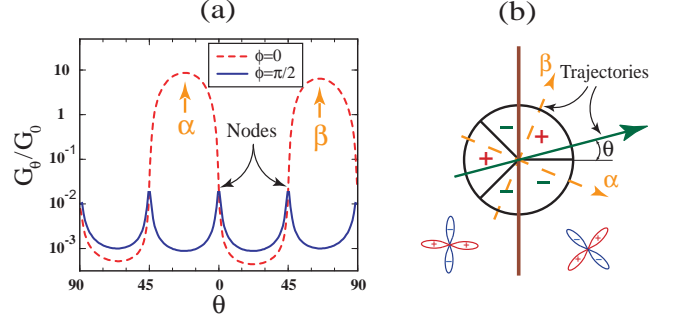


FIG. 1: (a) Angle resolved conductance, normalized to $G_0 = e^2 N_F v_F S$, for $\phi = 0$ (dashed line) and $\phi = \pi/2$ (solid line) at $T = 0.01T_c$. (b) Quasiparticle trajectories crossing the grain boundary. Trajectories along α and β directions see sign change of the order parameter. Other parameters are: $\omega = 0.02T_c$ and $\eta = 0.05T_c$.

is the contribution to the ac current density from a trajectory in θ direction (cf. Fig. 1b). Here $\hat{\tau}_3$ is the third Pauli matrix, $\hat{\mathbf{n}}$ is a unit vector in the direction of the trajectory ($\hat{\mathbf{n}} \cdot \hat{\mathbf{x}} = \cos\theta$), N_F is the density of states at the Fermi surface, and ϵ_c is an energy cutoff, which in our numerical calculations is taken to be $10T_c$. (The results however are insensitive to the exact value of ϵ_c .) The total conductance is given by $G = \int (d\theta/2\pi) G_\theta \cos\theta$.

Figure 1a shows G_θ for two values of phase difference ϕ across the junction. At $\phi = 0$, G is maximum at $\theta = -22.5^\circ$ and 67.5° (paths α and β in Fig. 1b). These are the directions along which the quasiparticles see different signs of the d -wave order parameter on either side of the boundary. Zero energy Andreev bound states formed in these directions are responsible for the large G [3]. Notice the asymmetry of G_θ with respect to $\theta = 0$ at $\phi = 0$. This asymmetry leads to an ac current parallel to the boundary [9]. The current vanishes at $\phi = \pi/2$ and is not dissipative (it is perpendicular to the electric field), therefore not central to our discussion.

A nonzero phase difference splits the bound states, moving them away from zero energy. Maximum splitting occurs at $\phi = \pi/2$. Nodal directions dominate the quasiparticle current at this phase difference (cf. Fig. 1a). Notice orders of magnitude difference in the conductance maxima between the two phase differences.

Figure 2a displays ϕ -dependence of the total G at two temperatures. Sharp peaks at $\phi = 0$ and π , 2–3 orders of magnitude larger than the minimum (at $\phi = \pi/2$), result from the MGS. The conductance spikes are much narrower at $T = 0.01T_c$ than at $0.1T_c$ and become extremely sharp at even lower T . As a result, the influence of the MGS is small at low T (see below). Figure 2b shows the T -dependence of G at $\phi = 0$ and $\pi/2$. While the two curves coincide at high T , they diverge as T is lowered. The conductance at $\phi = \pi/2$ is suppressed at low T . This is because the gapless quasiparticles on one

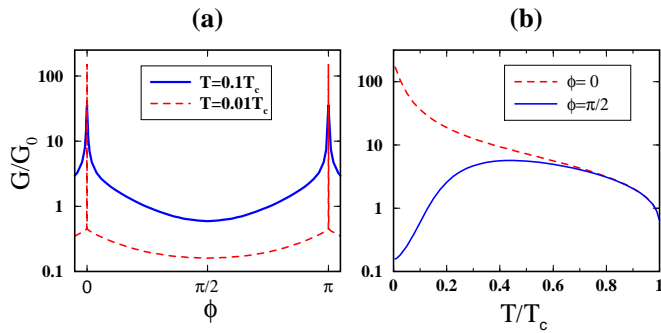


FIG. 2: ϕ (a) and T (b) dependence of G for the same set of parameters as in Fig. 1.

side of the junction see a gapped order parameter on the other side [17]. As $T \rightarrow 0$, however, it starts to saturate to a value almost proportional to η (see Fig. 3b). Similar behavior was also found for the case of superconducting point contacts [3].

To reduce decoherence, the qubit should be operated at low T . Figure 3 shows the ω and η dependence of G at $T = 10^{-4}T_c$. While strong ω -dependence of G exists at $\phi = 0$, it is almost frequency independent when $\phi = \pi/2$ (Fig. 3a). The η -dependence of G at $\phi = \pi/2$, on the other hand, is close to linear (Fig. 3b). The positive slope can be attributed to the broadening of the MGS with η , which enhances their overlap near zero energy, increasing their contribution to G .

We now try to calculate the decoherence time in a d -wave qubit, assuming a double well potential $U(\phi)$ with minima at $\pm\phi_0 \approx \pm\pi/2$. (A practical example of such a system is given in Ref. 6.) We first write down a Hamiltonian which, in classical regime, reproduces the above calculated G . At low frequencies, G shows slow ω -dependence for almost all ϕ (except for $\phi = 0, \pi$, which do not contribute to decoherence—see below). One can therefore assume our system to be coupled to an Ohmic heat bath [18]. To get a ϕ -dependent G , however, it is necessary to consider *nonlinear* coupling to the bath [19, 20] [see Eq. (13) below]. We therefore write the Hamiltonian as

$$H = \frac{Q^2}{2C} + U(\phi) - F(\phi)X, \quad (9)$$

where $Q = 2eP_\phi$ (P_ϕ momentum conjugate to ϕ) is the charge stored on the junction, and X is a heat bath operator. To find the relation between the nonlinear coupling function F and G , we first study the classical behavior of the above Hamiltonian. The equation of motion is

$$(C/4e^2)\ddot{\phi} = -\partial_\phi U(\phi) + \partial_\phi F(\phi)X, \quad (10)$$

Assuming small back-action of the system on the heat bath, one can use linear response theory [20] to write

$$X(t) = X^{(0)}(t) + \int dt' D(t-t')F[\phi(t')], \quad (11)$$

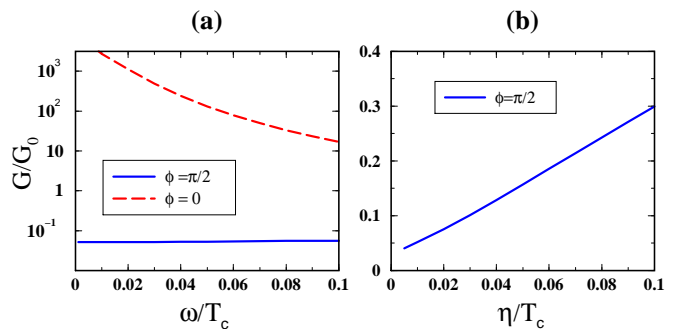


FIG. 3: Dependence of G on ω (a) and η (b) at $T = 10^{-4}T_c$. η in (a) and ω in (b) are equal to $0.01T_c$.

where $X^{(0)}$ is the unperturbed bath operator, $D(t-t') = \langle i[X^{(0)}(t), X^{(0)}(t')]_- \rangle \theta(t-t')$ is the bath's retarded Green's function, and $\langle \dots \rangle$ denotes equilibrium statistical averaging. For an Ohmic heat bath $D(t) = -\alpha\delta'(t)$ [in Fourier space $D(\omega) = i\alpha\omega$], with α being the dissipation coefficient and $\delta'(t)$ defined by $\int dt' \delta'(t-t')z(t') = \dot{z}(t)$.

Eq. (10) therefore leads to a stochastic equation that resembles the classical Langevin equation

$$(C/4e^2)\ddot{\phi} + \alpha(\partial_\phi F)^2 \dot{\phi} + \partial_\phi U = \xi_\phi, \quad (12)$$

where $\xi_\phi = (\partial_\phi F)X^{(0)}(t)$ is the fluctuation force [21]. The second term in (12) gives dissipation and therefore corresponds to the ϕ -dependent G [19]: $G(\phi) = 4e^2\alpha(\partial_\phi F)^2$. As a result

$$F(\phi) = \frac{1}{2e\sqrt{\alpha}} \int_0^\phi d\phi' \sqrt{G(\phi')}. \quad (13)$$

Notice the nonlocal dependence of F on G . The spike in G at $\phi = 0$ (cf. Fig. 2a) becomes extremely sharp as $T \rightarrow 0$, with little contribution to $F(\phi)$. This, although easily justified numerically, can be understood by making an analogy to the case of a superconducting point contact [3]: $G(\phi) \sim (\Delta/T)e^{-\Delta|\phi|/T}$ near the spike (ϕ measured from the center of the spike), leading to a contribution to $F(\phi)$ proportional to $\sqrt{T/\Delta}$, which is negligible as $T \rightarrow 0$. Numerical integration shows an even smaller effect.

In the quantum regime, one can truncate the Hilbert space to the left and right degenerate states, $|L\rangle, |R\rangle$, of the double-well potential, with $\langle L|F(\phi)|R\rangle \simeq 0$ and $\langle R|F(\phi)|R\rangle \simeq -\langle L|F(\phi)|L\rangle \simeq F(\phi_0)$. Equation (9) then gives the effective two-state Hamiltonian of the system (at the degeneracy), coupled to the heat bath, as

$$H_{\text{eff}} = -\frac{\delta E}{2}\sigma_x - F(\phi_0)X\sigma_z, \quad (14)$$

where δE is the energy splitting between the two lowest energy states of the system. The dephasing rate is proportional to the spectrum of heat bath fluctuations, $S(\omega) = \text{Im}[D(\omega)] \coth(\omega/2T)$, taken at the resonance frequency of the two-level system [see, e.g., Eq. (3.11) in

Ref. 18]. Then, the dephasing time τ_φ due to coupling to the Ohmic heat bath is obtained from

$$\tau_\varphi^{-1} = \alpha F(\phi_0)^2 \delta E \coth \frac{\delta E}{2T}. \quad (15)$$

Numerical calculation at $T = 10^{-4}T_c$ gives $\int_0^{\pi/2} \sqrt{G} d\phi \approx 0.38\sqrt{G_0}$, for $\eta = 0.01T_c$. Substituting into (13) and (15) and restoring \hbar , we find $\tau_\varphi^{-1} \approx 0.023R_QG_0\delta E/\hbar$, where $R_Q = h/(2e)^2 \approx 6.45 \text{ k}\Omega$ is the quantum resistance.

For quantitative estimation of τ_φ , we need to know the value of G_0 . We extract G_0 from the Josephson critical current density whose value is available from experiment [7]: $j_c \sim 10^2\text{--}10^4 \text{ A/cm}^2$. Our calculations at $T = 0.05T_c$ (close to 4.2K where most experiments are performed) show a critical current $I_c \approx 0.08G_0T_c/e$, almost independent of η . For a submicron junction of area $S \sim 0.01 \mu\text{m}^2$, we obtain (taking $T_c \approx 100 \text{ K}$) $G_0 \sim 10^{-5}\text{--}10^{-3} \text{ }\Omega^{-1}$. Assuming $\delta E/h \sim 1 \text{ GHz}$, we find $\tau_\varphi \sim 1\text{--}100 \text{ ns}$ (qubit quality factor $Q \sim 1\text{--}100$). Smaller η will result in a larger τ_φ . It is therefore desirable to use materials with low disorder and junctions with small roughness. Depending on the parameters, it is possible to observe signatures of quantum behavior (e.g. coherent tunneling), although the decoherence time may not be long enough for quantum computation.

Realistic junctions, in general, suffer from finite reflectivity, roughness, and faceting [22]. The effect of roughness, to some extent, is similar to that of η ; it broadens the MGS, increasing their contribution to G as they split [23]. Imperfect transparency also affects the MGS in a nontrivial way, influencing G . Presence of a subdominant order parameter at the junction, although yet unjustified experimentally [24], can enhance the quasiparticle resistance by opening a gap at the nodes. A small bulk size can also have a similar effect by quantizing momentum along the nodal directions. Most of the above mentioned effects can be studied within the framework of the present formalism and are the subject of further investigations.

Other sources, such as fluctuations of the external fields, coupling of bulk nodal quasiparticles to the electromagnetic field produced by the qubit (due to e.g. spontaneous currents), coupling to nuclear spins or paramagnetic impurities, background charge fluctuations, etc. will also contribute to the decoherence.

It is our pleasure to thank Ya. Fominov, A.A. Golubov, W.N. Hardy, Y. Imry, A. Maassen van den Brink, N. Schopohl, P.E.C. Stamp, and A.M. Zagoskin for helpful discussions, A.Ya. Tzalenchuk for experimental information, and A.J. Leggett for pointing out the necessity for nonlinear coupling to the heat bath.

- Yu *et al.*, Science **296** 889 (2002); J.M. Martinis *et al.*, Phys. Rev. Lett. **89** 117901 (2002); I. Chiorescu *et al.* Science **299**, 1869 (2003); E. Il'ichev *et al.*, Phys. Rev. Lett. **91**, 097906 (2003).
- [2] J.C. Cuevas, A. Martín-Rodero, and A.L. Yeyati, Phys. Rev. B **54**, 7366 (1996).
- [3] M.H.S. Amin, Phys. Rev. B **68**, 054505 (2003).
- [4] E. Il'ichev *et al.*, Phys. Rev. Lett. **86**, 5369 (2001).
- [5] L.B. Ioffe *et al.*, Nature (London) **398**, 679 (1999); A.M. Zagoskin, cond-mat/9903170; A. Blais and A.M. Zagoskin, Phys. Rev. A **61**, 042308 (2000).
- [6] M.H.S. Amin *et al.* preprint (cond-mat/0310224).
- [7] H. Hilgenkamp and J. Mannhart, Rev. Mod. Phys. **74**, 485 (2002).
- [8] A.Ya. Tzalenchuk *et al.*, Phys. Rev. B **68**, 100501(R) (2003).
- [9] M. Hurd *et al.*, Phys. Rev. B **59**, 4412 (1999).
- [10] U. Günsenheimer and A. D. Zaikin, Phys. Rev. B **50**, 6317 (1994).
- [11] See e.g. Yu.S. Barash, H. Burkhardt, and D. Rainer, Phys. Rev. Lett. **77**, 4070 (1996); M. Fogelström, D. Rainer, and J.A. Sauls, Phys. Rev. Lett. **79**, 281 (1997); W. Belzig, C. Bruder, and M. Sigrist, Phys. Rev. Lett. **80**, 4285 (1998).
- [12] N. Schopohl and K. Maki, Phys. Rev. B **52**, 490 (1995).
- [13] M.H.S. Amin, A.N. Omelyanchouk, and A.M. Zagoskin, Phys. Rev. B **63**, 212502 (2000); M.H.S. Amin *et al.*, Physica B **318**, 162 (2002); Phys. Rev. B **66**, 174515 (2002).
- [14] Here η is a phenomenological number to be extracted from experiment. It can also be calculated microscopically, taking into account electron-phonon and impurity scattering processes; the former makes it T -dependent.
- [15] Notice V_0 only appears in the calculation of G ; for decoherence calculation, no driving voltage is assumed (e.g. quantum beating). Even in the presence of a Rabi signal, since the Rabi frequency ω_R ($\sim eV_0$) is much smaller than ω ($= \delta E$), the condition can be easily met.
- [16] M. Eschrig, J.A. Sauls, and D. Rainer, Phys. Rev. B **60**, 10447 (1999); M. Eschrig, Phys. Rev. B **61**, 9061 (2000).
- [17] C. Bruder, A. van Otterlo, and G.T. Zimanyi, Phys. Rev. B **51**, 12904 (1995).
- [18] A.J. Leggett *et al.*, Rev. Mod. Phys. **59**, 1 (1987).
- [19] A.O. Caldeira, A.J. Leggett, Ann. Phys., **149**, 374 (1983).
- [20] G.F. Efremov and A.Yu. Smirnov, Sov. Phys. JETP, **53**, 547 (1981); A.Yu. Smirnov, Ann. Phys., **264**, 13 (1998).
- [21] In general $\langle \xi_\phi \rangle \neq 0$, and therefore (12) is not exactly the classical Langevin equation. When T is larger than the characteristic frequencies of the system, it is easy to show that $\langle \xi_\phi \rangle \approx 0$. At small T , however, it stays finite and adds nonvanishing quantum corrections to (12). Study of those are beyond the scope of the present article.
- [22] For small (submicron) junctions, faceting may only create uncertainty in the orientation of the boundary.
- [23] Ya.V. Fominov, A.A. Golubov, unpublished; Ya.V. Fominov, A.A. Golubov, and M.Yu. Kupriyanov, JETP Lett. **77**, 587 (2003).
- [24] W.K. Neils and D.J. Van Harlingen, Phys. Rev. Lett. **88**, 047001 (2002).

[1] Y. Nakamura, Yu. A. Pashkin, J. S. Tsai, Nature **398**, 786 (1999); D. Vion *et al.*, Science **296**, 886 (2002); Y.